Supplemental Information for "Urban Emissions and Regional Air Quality in India"

Alexandra Karambelas

1. Description of CMAQ Dust Module

Crustal species and resuspended dust were measured to contribute 17 to 56% of fine and coarse particulates in summertime [*Central Pollution Control Board,* 2011]. In Delhi and Kanpur to the east, summertime dust contributions average 10.25-14.3% and smaller amounts in the winter (3.9-6.8%) [*Behera and Sharma*, 2010; *Pant et al.*, 2015]. Large measured contributions, particularly in summertime suggest the importance of including windblown dust in model simulations. CMAQv5.0.1 includes a dust deflation module that can be turned on at the user's discretion and which was ultimately included for final presented simulations. The dust module calculates wind-blown dust emissions according to a system of equations incorporating land use fractions, wind speed, and soil moisture fraction as derived from MCIP [*Tong et al*., 2015]. Updates to the dust deflation module were incorporated for dust size mode speciation over Asia [*Dong et al.*, 2015]. Updated codes incorporated into CMAQ v5.0.1 were provided from Dr. Daniel Tong at the National Oceanic and Atmospheric Administration (NOAA).

Beyond source code updates, it was recommended by Dr. Tong (personal communication, February 2016) that additional factors may have to be adjusted to produce sufficient windblown dust. Using just the updates from Dr. Tong resulted in extremely minimal windblown dust changes, so we chose to adjust threshold friction wind velocity, u_t^*, to improve dust emissions over our domain. Suggestions for additional parameterization updates are provided in the discussion. Several factors impact u_t^*, which is calculated by the equation:

[1] $$u_t^* = u_t(F, l) * F_m$$

where u_t is the threshold friction velocity according to soil type (F) and land use type (l), and F_m is soil moisture. In the testing stages, we adjusted u_t^* twice, once to evoke significant amounts of dust and once to evoke moderate amounts of dust. We adjusted u_t^* by applying a multiplier of 1/10 (high dust) or 1/5 (low dust), effectively lowering the u_t^* and increasing the availability of dust uptake from the surface. The threshold friction velocity in CMAQ is dynamically calculated with assumptions about soil type, moisture content, and the presence of non-erodible elements. This leads to significantly lower average threshold friction velocity (0.07 ms^{-1}) than previously used or calculated for use in model studies over China (0.23-0.3 ms^{-1}) [*Dong et al.*, 2015; *Fu et al.,* 2014]. Final simulations for analysis include a moderate decrease in u_t^* because the extreme dust scenario resulted in unrealistic conditions specifically for the month of April.

2. Trend Analysis from Giovanni

Tropospheric column observations for NO_2, SO_2, and AOD for 2005, 2010, and 2015 are downloaded from the NASA Giovanni data portal in Level 3 format. VCDs for NO_2 and SO_2 are from OMI aboard the NASA Aura satellite. The Aura satellite is a polar-orbiting satellite with a local overpass time of about 1:30PM. OMI spatial footprint at 13 km by 24 km is small enough to capture changes between urban and non-urban areas. Measurements from OMI are important to assess atmospheric chemistry in the troposphere.

MODIS AOD measurements are helpful in assessing both urban and crustal (natural) pollution as well as pollution transport. Similar to OMI, the MODIS footprint is about 10 km at nadir. The MODIS instrument is on two satellites, Terra and Aqua; AOD presented here is from MODIS on Aqua. Aqua has an afternoon overpass time of about 1:30PM, coincident with OMI overpass time. Both OMI and MODIS have near daily global coverage. Cloud coverage can interfere with MODIS and OMI retrievals, limiting the availability of usable data. In India, this is common during the summer monsoon season, but the annual average obscures lost pixels during July. Giovanni allows detailed temporal from daily to multi-year scales. Annual average VCDs are presented for annual average to determine changes in pollution over time. Annual averages here will not indicate seasonal or incidents of transport, which can be evaluated under a higher temporal scale analysis.

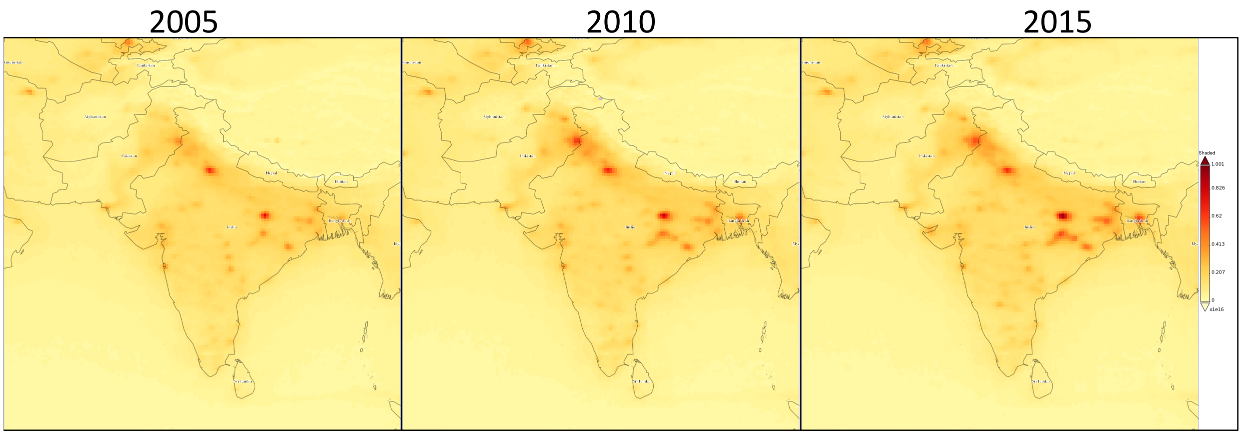

Figure SI 1 OMI tropospheric NO_2 for 2005 (left), 2010 (middle) and 2015 (right). Growth in NO_2 is evident in cities and industrial regions.

Annual average VCDs for NO_2, SO_2 and total AOD in 2005, 2010, and 2015 are shown in Figures SI 1-3. All three constituents show increases during this time period.

Greatest NO_2 VCDs are found in two locations across India: populated regions like Delhi and Mumbai, and industrial and electricity generating regions (Figure SI 1). Increases in NO_2 are noticeable across the region. Greatest VCDs of 10 x 10^{15} molecules per cm^2 or more can be found in Delhi (northwest) and Renukoot (east). Stack source emissions are highly noticeable by OMI in eastern India, which exhibit considerable growth and VCDs comparable and eventually surpassing those in Delhi. Largest growth is seen in the industrial east (i.e. Renukoot), which is evident in the increased NO_2 VCD locally and expansion spatially. Regions outside of India such as Dhaka in Bangladesh and Lahore in Pakistan also exhibit increases.

Similar to NO_2, SO_2 VCDs increase over time between 2005, 2010, and 2015 (Figure SI 2). Unlike NO_2, SO_2 is not predominant in cities. Instead, SO_2 VCDs are greatest in the industrial east. Visible

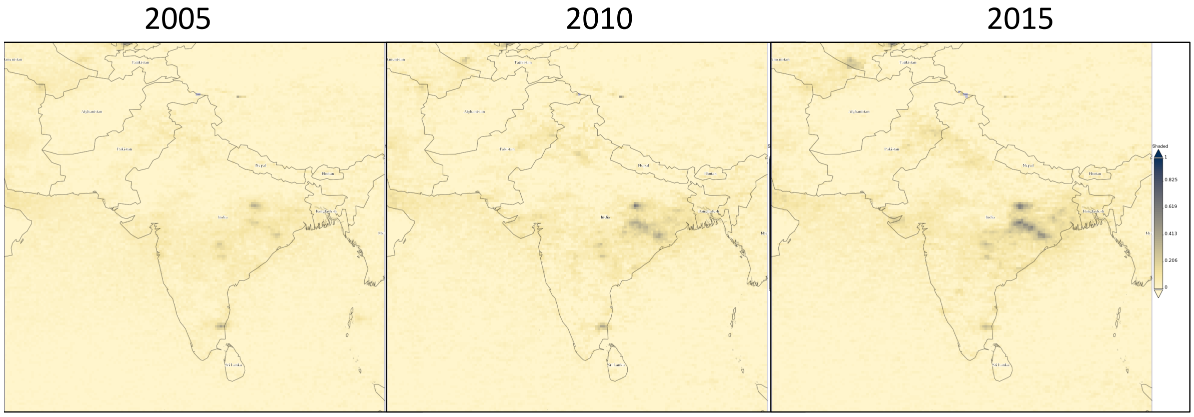

Figure SI 2 Same as Figure SI 1 except for OMI SO2.

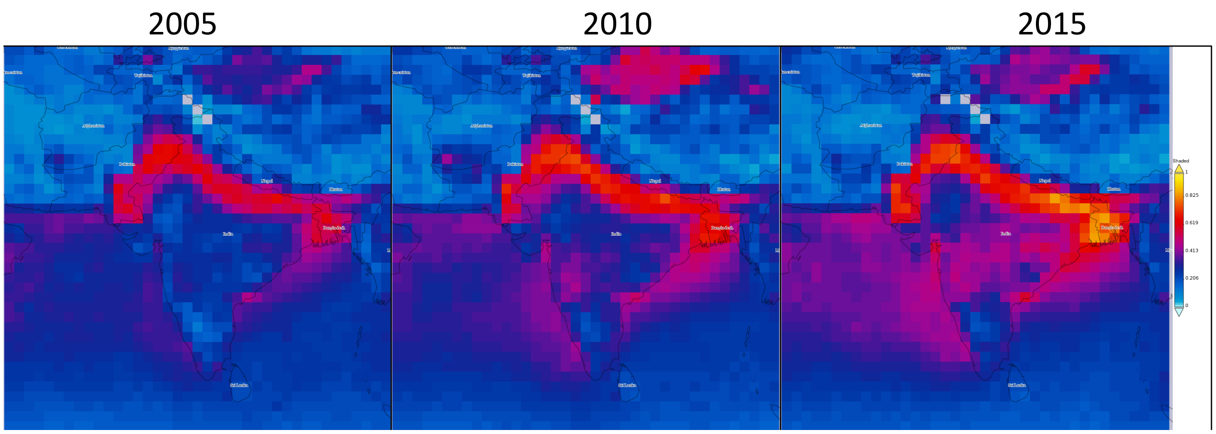

Figure SI 3 Same as Figure SI 1 except for AOD.

SO_2 VCDs are also found in central India near Hyderabad and along the south east coast south of Chennai. Greatest changes in SO_2 VCDs are found in the eastern industrial region, where SO_2 VCDs increase in magnitude and spatial coverage, suggesting growth in industry and electricity generation in the region between 2005 and 2015.

Finally, we assess AOD trends in India from 2005 to 2015 (Figure SI 3). AOD is sometimes used as a proxy for fine particulate matter, and it can be used to detect crustal and anthropogenic particles. Initially, AOD values are highest (0.4-0.6) along the Indo-Gangetic Plain near the Himalayas. This is coincident with greatest population density in India (not shown). AOD values are consistently lower across the central and southern parts of the country, around 0.2 or less, with an increase over Chennai on the east coast. Over time, AOD values increase considerably across the entire country. By 2015, AOD in central and southern India nearly double, and values in the north approach 1.0, most evident near Kolkata and the country of Bangladesh. Increases in AOD are likely connected to population growth, which increased by more than 150 million people during this time period, and is related to domestic biomass combustion.

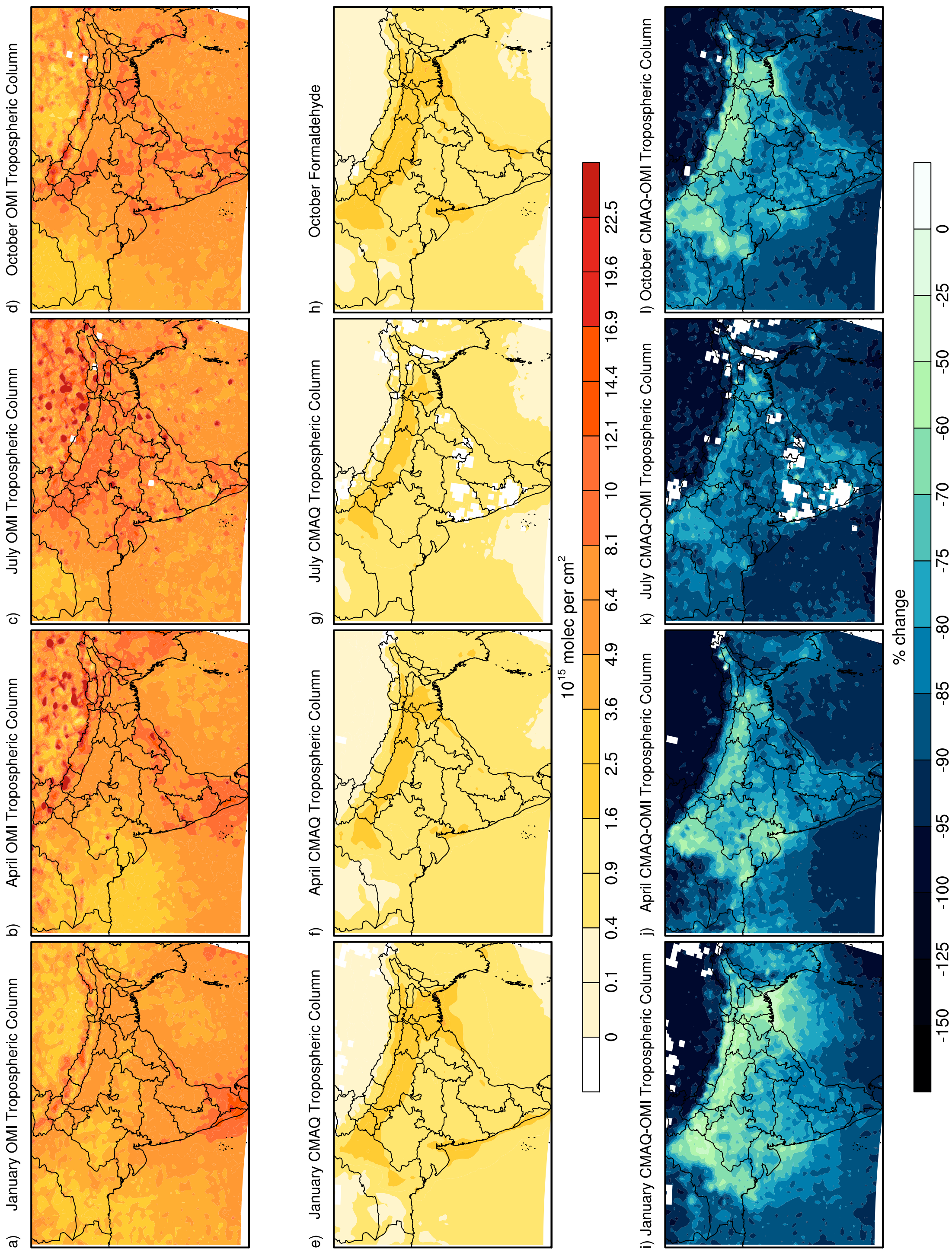

Figure SI 4 Same as Figure 1 except of satellite (a-d), modeled (e-h), and differences (i-l) for HCHO.

3. Tropospheric Column HCHO

Figure SI 4 presents a seasonal comparison of HCHO from OMI for satellite tropospheric columns (top), CMAQ tropospheric columns (middle) and the percent change between model and observations (bottom). Seasonal differences in tropospheric column HCHO are evident across India. In January, lowest HCHO is observed in the northwest, coincident with highest seasonal NO_2 (Figure SI 4a). July exhibits the highest observed HCHO, with column totals approaching values of 15 x 10^{15} molecules per cm^2 (Figure SI 4c). Values in southern India are consistently higher regionally for all four months. In comparison, modeled tropospheric columns are significantly lower regionally and seasonally (Figures SI 4e-h). Modeled seasonal variation is virtually nonexistent, and modeled total column HCHO remains less than 1 x 10^{15} molecules per cm^2 at maximum. Modeled total column HCHO is greatest in the Indo-Gangetic Plain along the Himalayas, and lowest in central and southern India, which is inconsistent with spatial distributions observed by OMI. Correspondingly, the greatest low model biases are found in central and southern India (Figures SI 4i-l). Biases in the form of percent change are lowest in northern India, where greatest tropospheric column HCHO exist. Statistics for model satellite HCHO comparison exhibit a weak correlation between modeled and measured tropospheric columns and significant low biases on average and seasonally (Table SI 1).

HCHO	Annual	January	April	July	October
r^2	0.10	0.12	0.09	0.07	0.24
NMB	-57.4%	-61.1%	-61.9%	-46.2%	-58.5%
NME	57.8%	61.8%	62.3%	46.4%	59.0%

Table SI 1 Same as Table 1 except showing statistical evaluation of CMAQ HCHO using OMI HCHO tropospheric columns.

4. References

Behera, S. N.; Sharma, M. Reconstructing Primary and Secondary Components of PM 2.5 Composition for an Urban Atmosphere. *Aerosol Sci. Technol.* **2010**, *44* (11), 983–992.

Central Pollution Control Board. *Air Quality Monitoring, Emission Inventory and Source Apportionment Study for Indian Cities*; 2011.

Dong, X.; Fu, J. S.; Huang, K.; Tong, D. Model Development of Dust Emission and Heterogeneous Chemistry within the Community Multiscale Air Quality Modeling System and Its Application over East Asia. *Atmos. Chem. Phys. Discuss.* **2015**, *15* (24), 35591–35643.

Fu, X.; Wang, S. X.; Cheng, Z.; Xing, J.; Zhao, B.; Wang, J. D.; Hao, J. M. Source, Transport and Impacts of a Heavy Dust Event in the Yangtze River Delta, China, in 2011. *Atmos. Chem. Phys.* **2014**, *14* (3), 1239–1254

Pant, P.; Shukla, A.; Kohl, S. D.; Chow, J. C.; Watson, J. G.; Harrison, R. M. Characterization of Ambient PM2.5 at a Pollution Hotspot in New Delhi, India and Inference of Sources. *Atmos. Environ.* **2015**, *109*, 178–189.

Tong, D. Q.; Bowker, G. E.; He, S.; Byun, D. W.; Mather, R.; Gillette, D. A. Development of a Windblown Dust Emission Model FENGSHAA Description and Initial Application in the United States. *Rev.* **2015**.